

Giant Magnetoimpedance Effect of Amorphous and Nanocrystalline Glass-Coated Microwires

A. Zhukov, A. Talaat, M. Ipatov, J.J. del Val, L. Gonzalez-Legarreta, B. Hernando and V. Zhukova

Abstract In this chapter we are reporting on correlation of Giant magnetoimpedance (GMI) effect and magnetic properties of amorphous and nanocrystalline Co-Fe rich glass-coated microwires. We measured the GMI magnetic field, frequency dependences and hysteresis loops of composite microwires produced by the Taylor-Ulitovsky technique. We observed that GMI effect and magnetic softness of glass-coated microwires produced by the Taylor-Ulitovsky technique can be tailored either controlling magnetoelastic anisotropy of as-prepared microwires or controlling their internal stresses and structure by heat treatment. High GMI effect has been observed in as-prepared and annealed Co-rich microwires. In the case of Fe-rich Finemet-type microwires we observed considerable magnetic softening of studied microwires after annealing. This magnetic softening correlates with the devitrification of amorphous samples. Amorphous Fe-rich microwires generally exhibited low GMI effect (GMI ratio below 5 %). Considerable enhancement of the GMI effect (GMI ratio up to 100 %) has been observed in heat treated microwires with nanocrystalline structure. The objective of this reported work is to develop magnetically soft thin wires for applications in magnetic field sensors.

A. Zhukov (✉) · A. Talaat · M. Ipatov · J.J. del Val · V. Zhukova
Department of Physics and Materials, Basque Country University, UPV/EHU,
San Sebastian, Spain
e-mail: arkadi.joukov@ehu.eus

A. Zhukov
IKERBASQUE, Basque Foundation for Science, Bilbao, Spain

L. Gonzalez-Legarreta · B. Hernando
Dpto de Física, Universidad de Oviedo, 33007 Oviedo, Spain

1 Introduction

Studies of Giant magnetoimpedance (GMI) effect attracted considerable during last two decades since its discovery in 1994 [1, 2]. It is worth mentioning that in fact GMI has been first reported in 1936 by Harrison et al. [3]. But intensive research of GMI effect in various materials began only after the publication in 1994 of a few papers on GMI effect in amorphous wires [4–8].

Phenomenologically, GMI effect consists of a large change of the impedance of a magnetically soft conductor under an applied magnetic field.

GMI effect is particularly interesting for magnetic sensors applications basically due to the extremely high magnetic field sensitivity suitable for low magnetic field detection [9, 10].

GMI effect has been successfully explained in the terms of classical electrodynamics through the influence of a magnetic field on the penetration depth of an electrical current flowing through the magnetically soft conductor [1, 2]. Cylindrical shape and high circumferential permeability observed in Co-rich amorphous wires with vanishing magnetostriction constant are quite favorable for achievement of high GMI effect [1, 2, 4].

The magnetic field dependence of impedance is intrinsically related to the magnetic anisotropy of magnetic materials [5, 7]. Magnetic materials with circumferential easy axis exhibit the maximum of the real component of wire impedance (and consequently of the GMI ratio) on magnetic field dependence. Although, magnetic materials with longitudinal easy axis present monotonic decay of the GMI ratio with increasing axial magnetic field, the maximum value of the GMI ratio corresponds to zero magnetic fields [5]. On the other hand, for optimization of the GMI effect, the magnetic anisotropy should be as small as possible.

The extremely high sensitivity of the GMI effect to even low magnetic field attracted a great interest in the field of applied magnetism, basically for applications for low magnetic field detection.

Usually, for the characterization of the GMI effect the magneto impedance ratio, $\Delta Z/Z$, is used. Aforementioned GMI ratio, $\Delta Z/Z$, is defined as:

$$\Delta Z/Z = [Z(H) - Z(H_{\max})]/Z(H_{\max}), \quad (1)$$

where H_{\max} is the applied axial DC-field with a maximum value up to a few kA/m.

Like the magnetic permeability, GMI effect has a tensor character [11–14]. From the point of view of industrial applications, the anti-symmetrical magnetic field dependence of the output voltage with a linear region obtained for pulsed GMI effect, that is based on the detection of the off-diagonal GMI component of amorphous wires is very suitable [5, 12]. Such pulsed scheme for GMI measurements results quite useful for real GMI sensors development [8].

The highest GMI effect is reported for the case of amorphous wires with high circumferential permeability [1, 2]. Moreover, after optimizing the magnetic anisotropy of Co-rich amorphous microwires a few researchers reported on an

achievement of about 600 % GMI ratio [15, 16]. The magnetic field dependence of the GMI ratio is mainly determined by the type of the magnetic anisotropy of the wire [5, 17]. Moreover, the AC and DC currents are the important parameters that affect the GMI effect. The main reason is that like magnetic permeability, GMI effect presents tensor character [13, 14]. The AC and DC currents flowing through the sample create a circumferential magnetic field. Additionally, the current produces Joule heating [18]. Depending on the frequency f of the driving AC current I_{ac} flowing through the sample, different GMI regimes can be considered:

1. At a low frequency range (1–10 kHz) the skin depth is usually larger than the radius or the sample (a rather weak skin effect). The impedance changes at these frequencies are of inductive character due to a circular magnetization process exclusively and might not be considered properly as the GMI effect.
2. At the frequency range from 10–100 kHz to 1–10 MHz (where the GMI effect has been first reported and described) the GMI originates basically from variations of the magnetic penetration depth due to strong changes of the effective magnetic permeability caused by a DC magnetic field [1, 2, 19]. It is widely believed that in this case both domain walls movement and magnetization rotation contribute to changes of the circular permeability and consequently to the skin effect.
3. For the MHz band frequencies (from 1–10 to 100–1000 MHz depending on the geometry of the sample), the GMI effect is also originated by the skin effect of the soft magnetic conductor, i.e. must be attributed to the GMI. But at these frequencies the domain walls are strongly damped. Therefore the magnetization rotation must be considered as responsible for the magnetic permeability change induced by an external magnetic field [1, 2, 19].
4. At GHz frequencies the magnetization rotation is strongly influenced by the gyromagnetic effect. With increasing the frequency the GMI peaks are shifted to higher magnetic fields values for being the sample magnetically saturated. At this frequency range, strong changes of the sample's impedance have been attributed to the ferromagnetic resonance (FMR) [20, 21].

It is also predicted that the diameter reduction must be associated with the increasing of the resonance frequency and therefore the increasing of the optimal GMI frequency range: a tradeoff between dimension and frequency is required in order to obtain a maximum effect [20].

Consequently, the major attention is recently focused on high frequencies (GHz range) GMI applications owing to the development of thin magnetically soft materials and the recent tendency in miniaturization of magnetic field sensors [7, 21].

Aforementioned GMI effect is considered as one of the most promising for applications in low magnetic field detection [8, 10, 22]. Magnetic sensors developed using amorphous wires with GMI effect allow achieving pT magnetic field sensitivity with low noise [22].

The aim of this chapter is to review recent efforts on the optimization of soft magnetic properties and GMI effect in amorphous and nanocrystalline glass-coated microwires fabricated by the Taylor-Ulitvosky technique.

2 Motivation

Nowadays, soft magnetic wires are considered as one of the most promising magnetic materials for industrial applications in various industrial sectors such as magnetic sensors, microelectronics, security, etc. [7, 9, 10, 19–22]. Extremely soft magnetic properties and Giant Magnetoimpedance effect are the features of magnetic wires that have been proposed for already existing and proposed industrial applications. Miniaturization of magnetic sensors requires reduction of the magnetic wires diameters. Thinnest magnetic wires can be produced using the Taylor-Ulitovsky method allowing the preparation of glass-coated microwires with metallic nucleus diameters from 0.05 to 50 μm coated by glass with a thickness ranging from 0.5 up to 30 μm . The fabrication method essentially consists in the melting of the metallic alloy ingot inside a glass tube and the rapid quenching from the melt of the metallic nucleus completely coated by the glass [4].

From the physical point of view, the interest in studying this kind of materials is related to its amorphous structure, therefore, such microwires are characterized by a low magnetic anisotropy (since the most important magneto-crystalline anisotropy is missing). Hence, their magnetic properties are determined mainly by the magnetoelastic and shape magnetic anisotropies. The latter can be significant if the microwire has thickest diameters (above 50 μm) in which the sample length affects their magnetic properties, particularly the hysteresis loop [4, 23]. Consequently, the main magnetoelastic anisotropy arises from the interaction of the local magnetic moments with the internal stresses induced during the microwire production, as well as from the difference between the thermal expansion coefficients of the metallic nucleus and the glass coating. Aforementioned magnetoelastic energy is given by:

$$K_{me} \approx 3/2 \lambda_s \sigma_i, \quad (2)$$

where λ_s is the saturation magnetostriction and σ_i is the internal stress. The magnetostriction constant depends mostly on the chemical composition and is vanishing in amorphous Fe-Co based alloys with Co/Fe \approx 70/5 [24–26].

The magnetic anisotropy of amorphous microwires in the absence of magnetocrystalline one has mostly a magnetoelastic origin, i.e., determined by the metallic nucleus composition and by the internal stresses [27–30]. The strength of internal stresses is mostly determined by the ratio, ρ , between the metallic nucleus diameter and total composite wire diameter, D ($\rho = d/D$). Such stresses arising during the simultaneous solidification of the composite wire originated from the

difference in thermal expansion coefficients of metallic alloy and glass coating [27–30] as has been above mentioned.

Consequently, the magnetic properties could be modified by either the heat treatment and/or chemical etching of the glass coating, or by selecting the adequate chemical composition of the metallic nucleus [4, 26].

On the other hand, it is well known that, the so-called “nanocrystalline materials”, that is, two-phase systems consisting of nano-sized grains randomly distributed in an amorphous matrix, attracted a great attention owing to extremely soft magnetic properties. These family of soft magnetic materials have been introduced in 1988, when Yoshizawa et al. [30], reported that the presence of small additions of Cu and Nb in certain Fe-Si-B alloys allows the creation of a two-phase material by the devitrification of the conventional amorphous alloy after adequate annealing (i.e., at temperatures between respective ones for the first and second crystallization processes) [30]. After crystallization, such material consists of small (around 10 nm grain size) nano-crystallites embedded in the residual amorphous matrix. In addition, the devitrification process of these amorphous alloys (with trademark FINEMET) leads to the possibility of obtaining rather different microstructures depending on the annealing parameters as well as on the chemical composition. These features are the basis to achieve the excellent soft magnetic properties indicated by a high value of permeability of about 10^5 , and correspondingly a low coercivity. Such soft magnetic character is thought to be originated because the magnetocrystalline anisotropy vanishes and a very small magnetostriction value results when the grain size approaches 10 nm [30–33]. As was theoretically estimated by Herzer [32, 33], the average anisotropy for randomly oriented α -Fe(Si) grains is negligibly small when grain diameter does not exceed about 10 nm. Thus, the resulting magnetic behavior can be well described with the random anisotropy model [32, 33]. According to this model, the low coercivity in the nanocrystalline state is ascribed to the small effective magnetic anisotropy K_{eff} around 10 J/m^3 .

GMI effect in amorphous microwires with positive magnetostriction constant exhibiting rectangular hysteresis loop is usually quite small because of their low initial permeability [34]. Recently, successful attempts for the improvement of GMI effect either by nanocrystallization of amorphous precursor or by induction of a transverse easy magnetization direction under special heat treatment (under stress and/or magnetic field) have been reported [34–38].

Meanwhile, substitution of Co-rich amorphous microwires by less expensive Fe-rich microwires can be essentially promising from industrial application’s point of view. Therefore, optimizing high GMI effect in Fe-rich glass-coated microwires is nowadays one of the major subjects of research.

In this chapter we present our last results on optimization of GMI effect in amorphous and nanocrystalline glass-coated microwires. This will help in improving the sensitivity of the magnetic sensors based on GMI effect.

3 Tuning of GMI Effect in Amorphous Glass-Coated Microwires

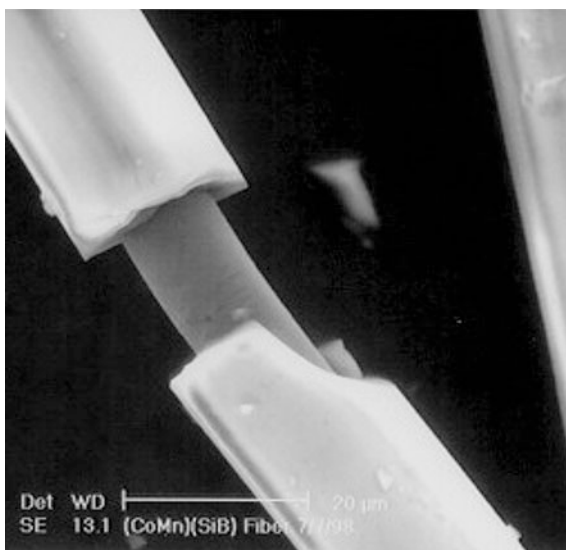
As mentioned above, the development of thin soft magnetic wires with amorphous and nanocrystalline structure is essential for the creation of magnetic sensors based on GMI effect. Therefore, the understanding of the main factors affecting magnetic properties of thin wires is of critical importance for the optimization of their magnetic properties.

The Taylor-Ulitovsky method allows producing of thinnest metallic wires (with typical diameters of the order of 1–30 μm) covered by an insulating glass coating [23, 26]. In fact, this method is known from many years [39–42], but since the 90s it has been widely employed for fabrication of ferromagnetic amorphous microwires coated by glass (see photo in Fig. 1). The fabrication method denominated in most of modern publications as a modified Taylor-Ulitovsky and/or quenching-and-drawing method is actually well-known since the 60s and well described in Russian in 60s [39–41] as well as in more recent publications [26, 42].

As described elsewhere the fabrication method consists of melting of an ingot containing a few grams of the master alloy with the desired composition placed into a Pyrex-like glass tube inside a high frequency inductor heater. Once the alloy is heated up to its melting point, forming a droplet and a glass capillary is then drawn from the softened glass portion and wound on a rotating spool. At suitable drawing conditions, the molten metal fills the glass capillary and a microwire is thus formed where the metal core is completely coated by the glass shell [4, 23, 26].

The microstructure of the microwire (and consequently its magnetic properties) depends mainly on the cooling rate. Chemical and metallurgical processes related to

Fig. 1 Micrograph of the glass-coated microwire. Reprinted with permission from [26] (Fig. 2)



the interaction of the ingot alloy and the glass, electromagnetic and electro-hydrodynamic phenomena in the system of inductor-ingot, thermal conditions of formation of cast microwire, casting process parameters and their limits affecting the casting rate and the diameter of the microwire were described in details for non-magnetic microwires [39–41] and overviewed in a relatively recent book [43]. From the point of view of magnetic properties of thin magnetic microwires and properties related to its surface layers (like is the case of GMI effect), the interfacial layer between the metallic nucleus and glass coating is especially relevant [43]. The features of the interfacial layer between the metallic nucleus and glass coating (its thickness, structure and physical properties) depend on the origin of the interfacial layer. Thus, the thickness of the interfacial layer might have from a few μm for the case of the formation of series of solid solutions or stable chemical compounds, to less than 0.1 μm in the case of the origin related to the uncompensated molecular forces on the interface between the glass and the metallic nucleus [43]. Recently an interfacial layer thickness for the case of Fe-rich microwires of about 0.5 μm has been reported [44].

The other source of instability of properties of as-prepared microwires is related to the gas content inside the microwire. The sources of the gas are: the atmosphere, gas impurities in the alloy and in the glass [43, 44].

The great advantage of these microwires is that the obtained diameter could be significantly reduced in comparison with the case of amorphous wires produced by the in-rotating water method. But their magnetic properties are also quite different from “thicker” amorphous wires. Thus although like in the case of “thicker wires” it was observed that Fe-rich compositions with positive magnetostriction constant show generally rectangular hysteresis loop, Co-rich negative magnetostrictive compositions present a completely different character of hysteresis loops. Co-rich microwires have almost non-hysteretic magnetization curves and glass coating removal results in the appearance of magnetic bistability [4, 23, 26, 43]. This is because the glass coating introduces additional internal stresses due to the difference between the thermal expansion coefficients of glass coating and metallic nucleus. Therefore, microwires of the same composition can show different magnetic properties arising from different magnetoelastic energy.

As already mentioned in the introduction, the GMI effect usually observed in soft magnetic materials phenomenologically consists of the change of the AC impedance, $Z = R + iX$ (where R is the real part, or resistance, and X is the imaginary part, or reactance), when submitted to an external magnetic field, H_0 . The GMI effect was well interpreted in terms of the classical skin effect in a magnetic conductor assuming the dependence of the penetration depth of the AC current flowing through the magnetically soft conductor on the DC applied magnetic field [1, 2].

The electrical impedance, Z , of a magnetic conductor in this case is given by [14–16]:

$$Z = R_{dc}krJ_0(kr)/2J_1(kr) \quad (3)$$

with $k = (1 + j)/\delta$, where J_0 and J_1 are the Bessel functions, r is the wire's radius and δ the penetration depth given by:

$$\delta = \sqrt{\pi\sigma\mu_\phi f} \quad (4)$$

where σ is the electrical conductivity, f the frequency of the current along the sample, and μ_ϕ the circular magnetic permeability assumed to be scalar. The DC applied magnetic field introduces significant changes in the circular permeability, μ_ϕ . Therefore, the penetration depth also changes through and finally results in a change of Z [1, 2].

In ferromagnetic materials with high circumferential anisotropy (the case of magnetic wires) the magnetic permeability possesses the tensor nature and the classic form of impedance definition is no valid. The relation between electric field (which determines the voltage) and the magnetic field (which determines the current) is defined through the surface impedance tensor [11, 12]

$$e = \hat{\zeta}h \quad \text{or} \quad \left\{ \begin{array}{l} e_z = \zeta_{zz}h_\phi - \zeta_{z\phi}h_z \\ e_\phi = \zeta_{\phi z}h_\phi - \zeta_{\phi\phi}h_z \end{array} \right\} \quad (5)$$

The circular magnetic fields h_ϕ is produced by the currents i_w running through the wire. At the wire surface $h_z = i/2\pi r$, where r is the wire radius. The longitudinal magnetic fields h_z is produced by the currents i_c running through the exciting coil, $h_z = N_1 i_c$, where N_1 is the exciting coil number of turns.

Various excitation and measurement methods are required to reveal the impedance matrix elements. The longitudinal and circumferential electrical field on the wire surface can be measured as voltage drop along the wire v_w and voltage induced in the pickup coil v_c wound on it [11, 12, 26, 45].

$$v_w \equiv e_z l_w = (\zeta_{zz}h_\phi - \zeta_{z\phi}h_z)l_w \quad (6)$$

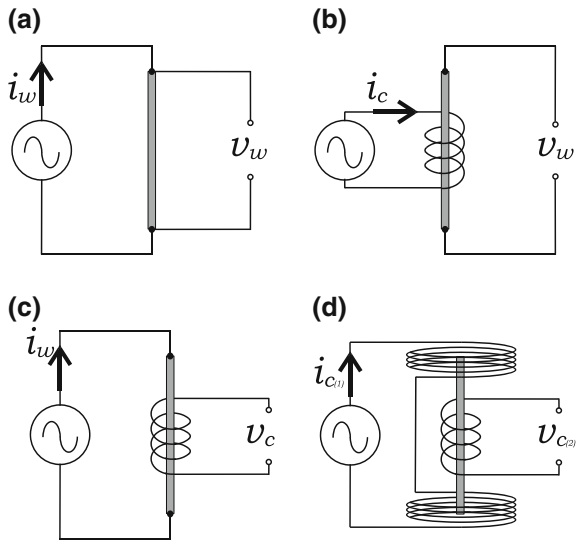
$$v_c \equiv e_\phi l_t = (\zeta_{\phi z}h_\phi - \zeta_{\phi\phi}h_z)l_t \quad (7)$$

where l_w is the wire length, $l_t = 2\pi r N_2$ the total length of the pickup coil turns N_2 wound directly on the wire.

The methods for revealing the different elements of impedance tensor are shown in Fig. 2. The longitudinal diagonal component ζ_{zz} is defined as the voltage drop along the wire and corresponds to impedance definition in classical model (Fig. 2a).

$$\zeta_{zz} \equiv \frac{v_w}{h_\phi l_w} = \left(\frac{2\pi a}{l_w} \right) \left(\frac{v_w}{i_w} \right) \quad (8)$$

Fig. 2 Methods for revealing the impedance matrix elements: **a** ζ_{zz} , **b** $\zeta_{z\varphi}$, **c** $\zeta_{\varphi z}$, **d** $\zeta_{\varphi\varphi}$. Reprinted with permission from [14] DOI 10.1002/pssa.200778133, Copyright © 2008 WILEY-VCH Verlag GmbH & Co. KGaA, Weinheim (Fig. 1)



The off-diagonal components $\zeta_{z\varphi}$ and $\zeta_{\varphi z}$ (Fig. 2b, c) and the circumferential diagonal component $\zeta_{\varphi\varphi}$ (Fig. 2d) arose from cross sectional magnetization process ($h_\varphi \rightarrow m_z$ and $h_z \rightarrow m_\varphi$) [11, 12, 26, 45].

From the point of view of industrial applications low hysteretic GMI effect with linear magnetic field dependence of the output signal are desirable [11, 12]. Anti-symmetrical magnetic field dependence of the output voltage with linear region has been obtained for a pulsed GMI effect based on the detection of the off-diagonal GMI component of amorphous wires [11, 12, 45]. Such pulsed scheme for GMI measurements resulted quite useful for real GMI sensors development [11, 12].

As mentioned above, the shape of magnetic field dependence of the GMI effect (including off-diagonal components) is intrinsically related to the magnetic anisotropy and the peculiar surface domain structure of amorphous wires [4, 5]. Magnetic anisotropy of amorphous microwires in the absence of magnetocrystalline anisotropy is determined mostly by the magnetoelastic contribution [4, 26]. As mentioned above, the internal stresses, σ_i , arising during simultaneous rapid quenching of metallic nucleus surrounding by the glass coating are the source of additional magnetoelastic anisotropy. The strength of such internal stresses can be controlled by the ρ -ratio. The strength of internal stresses increases with the decreasing of ρ -ratio (i.e., increases with the increasing of the glass volume) [27–29].

We measured magnetic field dependences of impedance, Z , and GMI ratio, $\Delta Z/Z$, for various as-prepared and annealed Co- and Fe-rich microwires.

A Schematic picture showing principles for revealing the impedance matrix elements: diagonal, ζ_{zz} , and off-diagonal, $\zeta_{z\varphi}$, is shown in Fig. 3.

We used a specially designed micro-strip sample holder (see the image in Fig. 3b). The microwire was placed inside a sufficiently long solenoid that creates a

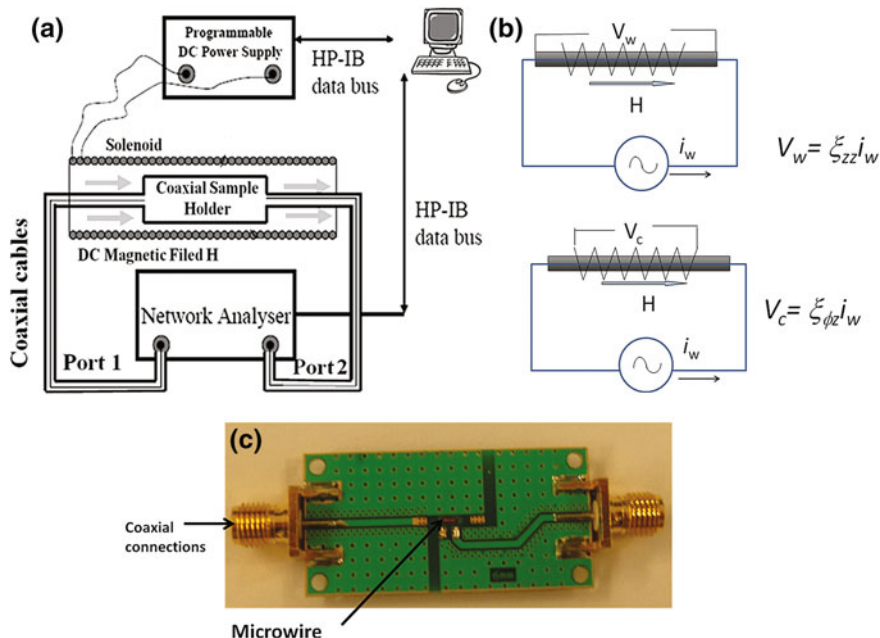


Fig. 3 Schematic picture of the experimental set-up for measurements of GMI effect (a), principles for revealing of the diagonal, ξ_{zz} , and off-diagonal, $\xi_{\phi z}$, impedance matrix elements (b) and the image of the micro-strip line (c). Reprinted with permission from [46], International Journal on Smart Sensing and Intelligent Systems, Copyright © 2014 (Fig. 3)

homogeneous magnetic field H . The sample impedance Z was measured using a vector network analyzer from the reflection coefficient S_{11} . The DC bias current I_B was applied to the sample through a bias-tee element. All experimental graphs show both ascending and descending branches of the field dependencies of the real part of impedance Z so that the magnetic hysteresis can be evaluated. More details on experimental technique can be found in Refs. [46–48].

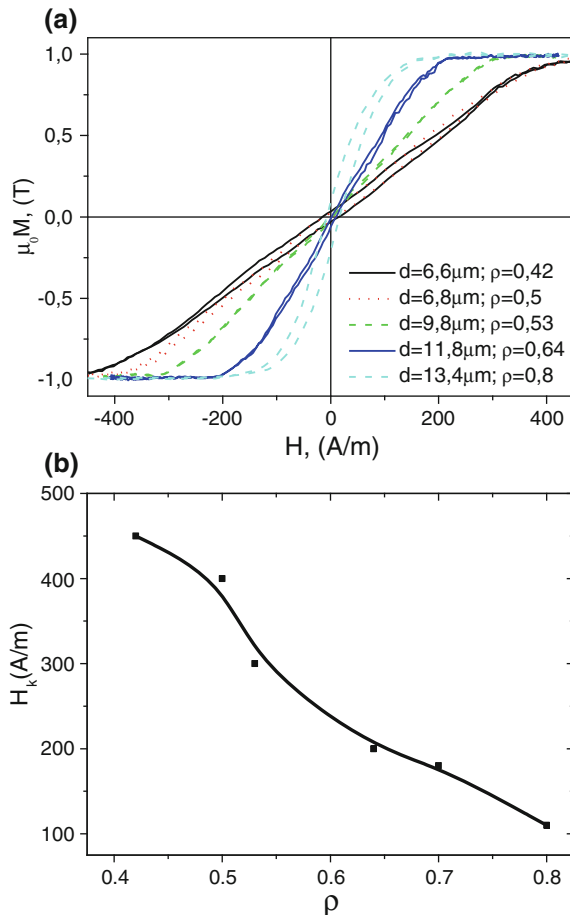
Below we overview a few recent results on GMI effect in microwires paying attention on its suitability for magnetic sensors applications.

It is worth mentioning, that usually the DC magnetic field that corresponds to the maximum GMI ratio, H_m , is attributed to the static magnetic anisotropy field, H_k . Consequently, the parameter ρ must be considered as one of the factors that affect both soft magnetic properties and GMI response.

Figure 4 shows the influence of the ρ -ratio on hysteresis loops and magnetic anisotropy field of $\text{Co}_{67.1}\text{Fe}_{3.8}\text{Ni}_{1.4}\text{Si}_{14.5}\text{B}_{11.5}$ microwires with the same composition of the metallic nucleus, but different ρ -ratio.

As can be appreciated, Co-rich microwire with appropriate geometry and composition present excellent magnetically soft properties with low coercivities (between 4 and 10 A/m) [4, 23, 26, 48]. Magnetic anisotropy field, H_k , is found to

Fig. 4 Hysteresis loops of $\text{Co}_{67.1}\text{Fe}_{3.8}\text{Ni}_{1.4}\text{Si}_{14.5}\text{B}_{11.5}\text{Mo}_{1.7}$ microwires with different geometry (a) and dependence of H_k on ρ -ratio (b). Reprinted with permission from [48], DOI: [10.1051/epjconf/20122900052](https://doi.org/10.1051/epjconf/20122900052), Owned by the authors, published by EDP Sciences, 2012 (Fig. 4)



be determined by the ρ -ratio, decreasing with ρ (Fig. 4b), as has been reported elsewhere [23, 26].

Consequently, one can expect that the ρ -ratio must affect the GMI effect of studied samples.

Figure 5 presents results on magnetic field dependences of ΔZZ measured in Co-rich microwire samples with different ρ -ratios.

Indeed both maximum values of the GMI ratio, ΔZZ_m , and the magnetic anisotropy field present a considerable dependence on the samples geometry. It is worth mentioning, that for microwires with the lowest glass coating thickness (largest ρ -ratio) a value of $\Delta ZZ_m \approx 600\%$ has been observed [23, 26]. Considering that the magnetoelastic energy, K_{me} , is determined by both internal, σ_i , and applied stresses, σ_a , the GMI effect has been measured under tensile stresses in various Co-rich microwires. Figure 6 presents tensile stress dependence measured in $\text{Co}_{67.05}\text{Fe}_{3.85}\text{Ni}_{1.4}\text{B}_{11.33}\text{Si}_{14.47}\text{Mo}_{1.69}$ and $\text{Co}_{68.5}\text{Mn}_{6.5}\text{Si}_{10}\text{B}_{15}$ microwires. It was

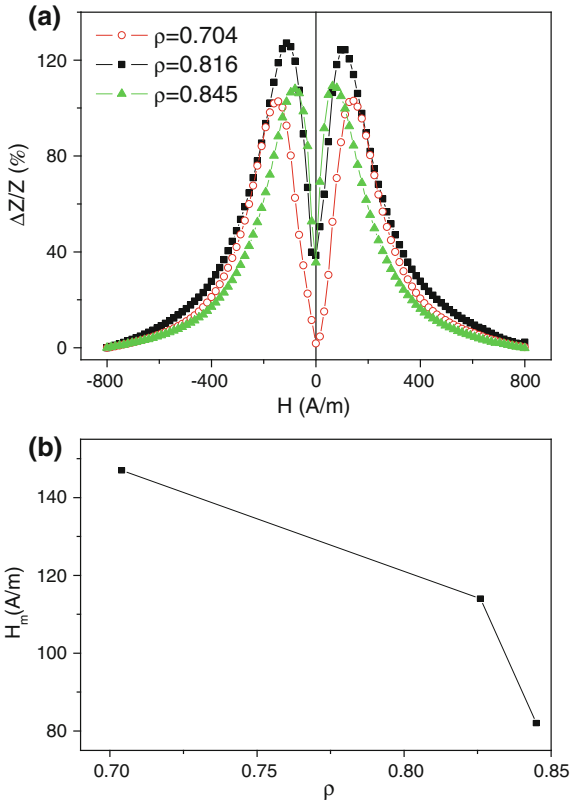


Fig. 5 Effect of ρ -ratio on GMI effect in $\text{Co}_{67.05}\text{Fe}_{3.85}\text{Ni}_{1.4}\text{B}_{11.33}\text{Si}_{14.47}\text{Mo}_{1.69}$ microwire samples with different ρ -ratios (a, b) and dependence of field of maximums on ρ -ratio (c). Reprinted with permission from Ref. [21] DOI 10.1007/s10948-012-1962-x, Copyright (2013) with permission from Springer (Fig. 6)

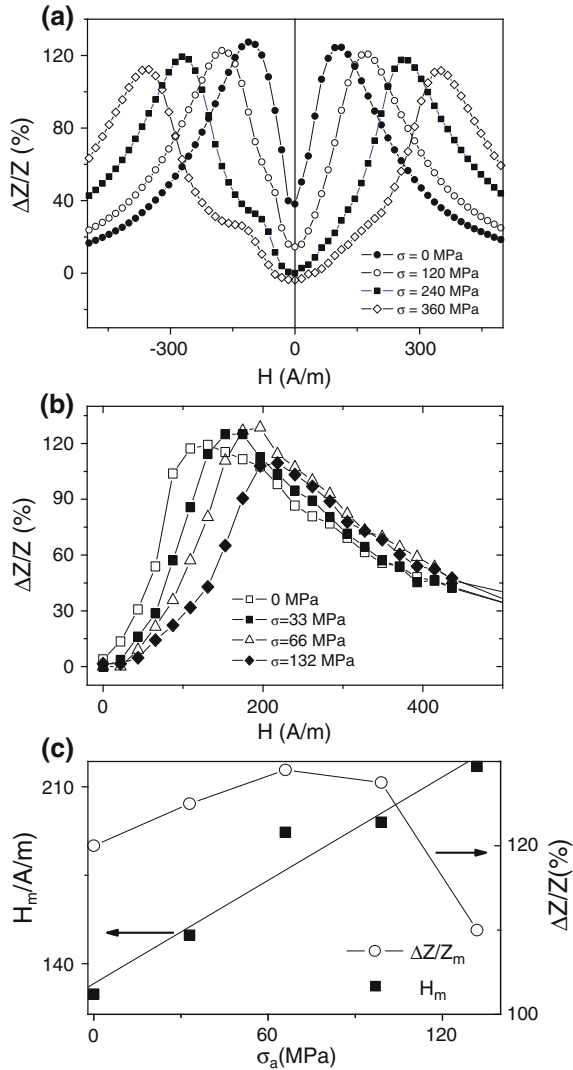
observed, that $\Delta Z/Z$ and H_m are quite sensitive to the application of external tensile stresses, σ_a : here the magnetic field, H_m corresponding to the maximum of $(\Delta Z/Z)$ shows a roughly linear increase with σ (Fig. 6c).

As mentioned above, the value of the DC axial field H_m , that corresponds to the maximum GMI ratio should be attributed to the static circular anisotropy field, H_k . This argument allows us to estimate the magnetostriction constant using the dependence $H_m(\sigma)$ presented in the Fig. 6c and the well known expression for the stress dependence of anisotropy field [23, 24, 49], given by

$$\lambda_s = (\mu_o M_s / 3)(dH_k / d\sigma), \quad (9)$$

where $\mu_o M_s$ is the saturation magnetization.

Fig. 6 $\Delta Z/Z(H)$ dependences of $\text{Co}_{67.05}\text{Fe}_{3.85}\text{Ni}_{1.4}\text{B}_{11.33}\text{Si}_{14.47}\text{Mo}_{1.69}$ (a) and $\text{Co}_{68.5}\text{Mn}_{6.5}\text{Si}_{10}\text{B}_{15}$ (b) amorphous microwires measured at different σ_a and $H_m(\sigma)$ dependence for $\text{Co}_{68.5}\text{Mn}_{6.5}\text{Si}_{10}\text{B}_{15}$ amorphous microwire (c). Reprinted with permission from Ref. [21] DOI [10.1007/s10948-012-1962-x](https://doi.org/10.1007/s10948-012-1962-x), Copyright (2013) with permission from Springer (Fig. 7)



A comparison with the reported values measured from the stress dependence of initial magnetic susceptibility ($\lambda_{s,0} \approx -3 \times 10^{-7}$ for such composition) and the magnetostriction values measured in amorphous wires of similar compositions has been reported [49].

In fact, the tendency on the change of H_m under the application of tensile stresses (Fig. 6c) and the change of H_m and H_k with the decreasing of the ρ -ratio (Figs. 4, 5 and 6) is the same confirming then the effect of magnetoelastic anisotropy on hysteresis loops and GMI effect.

The $H_m(\sigma)$ dependence (see the Fig. 6c) exhibits a slope of around $0.7 \text{ A}/(\text{m} \times \text{MPa})$, that allows an estimation of the unstressed value of the saturation magnetostriction constant, $\lambda_{s,0}$. The estimated value for $\lambda_{s,0}$ was -2×10^{-7} , which is rather reasonable for the studied samples.

According to the usual definition, the complex impedance of a linear electronic element at the circular frequency ω is given by:

$$Z(\omega) = U_{ac}/I_{ac} = Z_1 + iZ_2, \quad (10)$$

where I_{ac} is the harmonic current with frequency ω flowing through the element and U_{ac} is the harmonic voltage of the same frequency, measured between its terminals [1, 2].

In fact as has been already mentioned, see for example [11], the Eq. (10) is not fully applicable to ferromagnetic conductors because usually such materials are not linear. This occurs because U_{ac} is generally not proportional to I_{ac} and it is not a harmonic function of time (it contains higher order harmonics) [11, 46].

Additionally, although widely used, the definition of the GMI ratio $\Delta Z/Z$, mentioned above, may be useful for quantifying the huge attained variations of impedance, but the information about the phase shift is lost; it depends on the ambiguously chosen H_0 max (although the sample might be apparently magnetically saturated it does not mean that GMI is also saturated). But in any case, most of published papers use $\Delta Z/Z$ or longitudinal impedance change when the frequency dependence of GMI effect is studied.

The magnetic field dependence of real part Z_1 of the longitudinal wire impedance Z_{zz} ($Z_{zz} = Z_1 + iZ_2$), measured up to 4 GHz in $\text{Co}_{66}\text{Cr}_{3.5}\text{Fe}_{3.5}\text{B}_{16}\text{Si}_{11}$, $\text{Co}_{67}\text{Fe}_{3.85}\text{Ni}_{1.45}\text{B}_{11.5}\text{Si}_{14.5}\text{Mo}_{1.7}$ and $\text{Co}_{67.71}\text{Fe}_{4.28}\text{Ni}_{1.57}\text{Si}_{11.24}\text{B}_{12.4}\text{Mo}_{1.25}\text{C}_{1.55}$ microwires is shown in Fig. 7. The general feature of this dependence is that the magnetic field value corresponding to the maximum impedance shifts to the higher field region with the increasing f . A high enough magnetic field sensitivity, i.e., GMI effect till GHz- range frequencies should be also underlined. On the other hand, if the maximum applied magnetic field is not high enough, impedance change induced by applied magnetic field at high frequencies starts to decrease at some frequency. For example, most of the microwires show the highest GMI ratio at frequencies between 100 and 300 MHz (see for example Fig. 8 for $\text{Co}_{66.87}\text{Fe}_{3.66}\text{C}_{0.98}\text{Si}_{11.47}\text{B}_{13.36}\text{Mo}_{1.52}$ microwires). Another interesting features observed in Fig. 8a, b are that the frequency dependence of maximum GMI ratio, $\Delta Z/Z_m(f)$, measured in microwires of the same composition with different diameters presents an optimum frequency (at which $\Delta Z/Z_m$ versus f exhibits the maximum) at different frequency values. Thus, for metallic nucleus diameters ranging between 8.5 and 9.0 μm , the optimal frequency is about 100 MHz, while for microwires with metallic nucleus diameters between 9 and 11.7 μm , the optimal frequency is about 200 MHz.

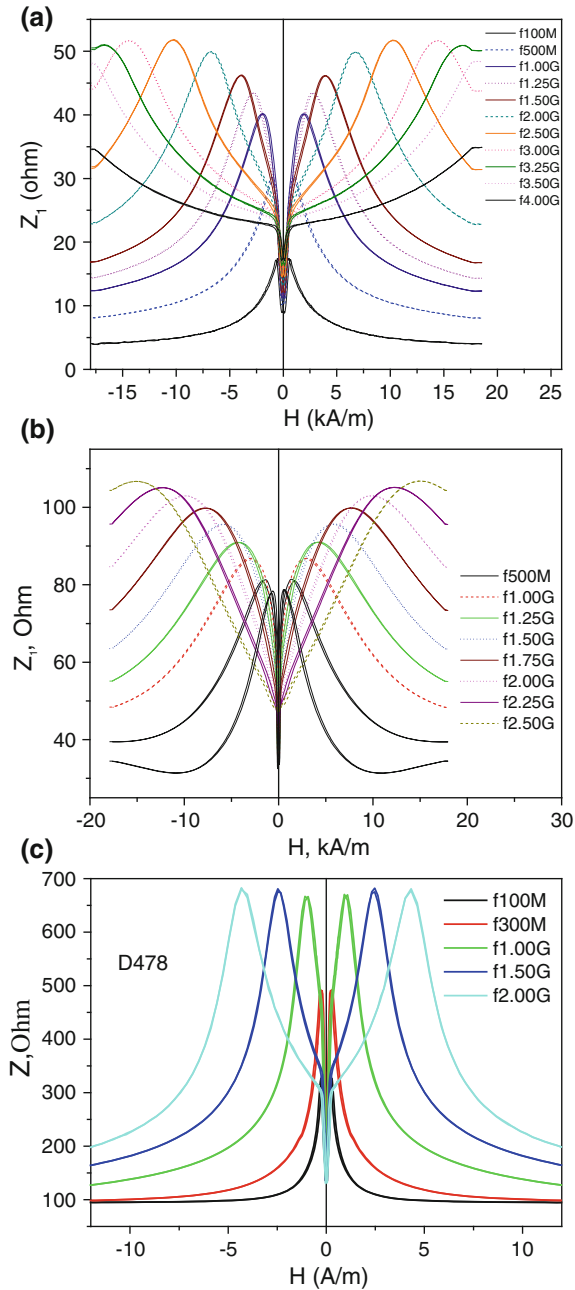


Fig. 7 $Z(H)$ dependences of $\text{Co}_{66}\text{Cr}_{3.5}\text{Fe}_{3.5}\text{B}_{16}\text{Si}_{11}$ (a) $\text{Co}_{67}\text{Fe}_{3.85}\text{Ni}_{1.45}\text{B}_{11.5}\text{Si}_{14.5}\text{Mo}_{1.7}$ (b) and $\text{Co}_{67.71}\text{Fe}_{4.28}\text{Ni}_{1.57}\text{Si}_{11.24}\text{B}_{12.4}\text{Mo}_{1.25}\text{C}_{1.55}$ (c) microwires measured at different frequencies. Reprinted with permission from [46], Copyright©2014, with permission from International Journal on Smart Sensing and Intelligent Systems, <http://www.s2is.org>, (Fig. 5)

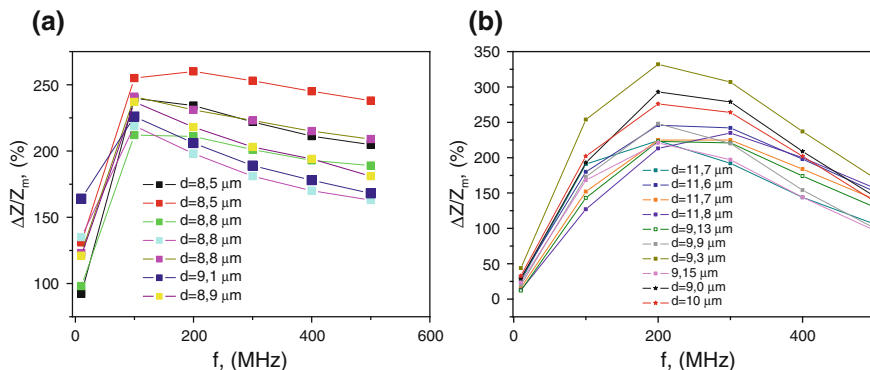


Fig. 8 Frequency dependence of ΔZZ_m in $\text{Co}_{66.87}\text{Fe}_{3.66}\text{C}_{0.98}\text{Si}_{11.47}\text{B}_{13.36}\text{Mo}_{1.52}$ microwires with different metallic nucleus diameters. Reprinted with permission from [7], Copyright (2014), with permission from Elsevier, doi:10.1016/j.jallcom.2012.10.082 (Fig. 5)

As regarding to the origin of the frequency dependence of H_m , observed in Fig. 8 for both microwires, there are different points of view. Experimentally, it has been observed that the magnetic field at which the maximum occurs considerably increases with the frequency (Fig. 7).

One possible explanation for this fact is that the magnetic domain structure and the anisotropy can be different near the surface. At higher frequencies the current flows closer to the surface, then the effective anisotropy field and dispersion can change with the frequency. Another reason might be connected with the frequency dependence of the domain wall permeability and aforementioned FMR contribution at higher frequencies.

The close analogy between the giant magnetoimpedance and ferromagnetic resonance has been previously reported elsewhere [20, 46, 50, 51]. Indeed the saturation magnetization M_s can be estimated from the equation:

$$M_s = 0.805 \times 10^{-9} df_0^2/dH \quad (11)$$

where f_0 is the resonant frequency and H is the applied magnetic field. This approach predicts the linear relation between the square of the resonance frequency as a function of the applied field, $f_0^2(H)$. The experimental data for GMI effect measured in $\text{Co}_{67.05}\text{Fe}_{3.85}\text{Ni}_{1.4}\text{B}_{11.33}\text{Si}_{14.47}\text{Mo}_{1.69}$ microwires fits well with the predicted linear dependence (see Fig. 9).

The saturation magnetization values, obtained from (11) give us quite reasonable values of about 0.5–0.53 MA/m. Consequently frequency dependence of GMI effect at GHz frequencies fits well with the ferromagnetic resonance behaviour, as has been previously reported elsewhere [46, 50, 51].

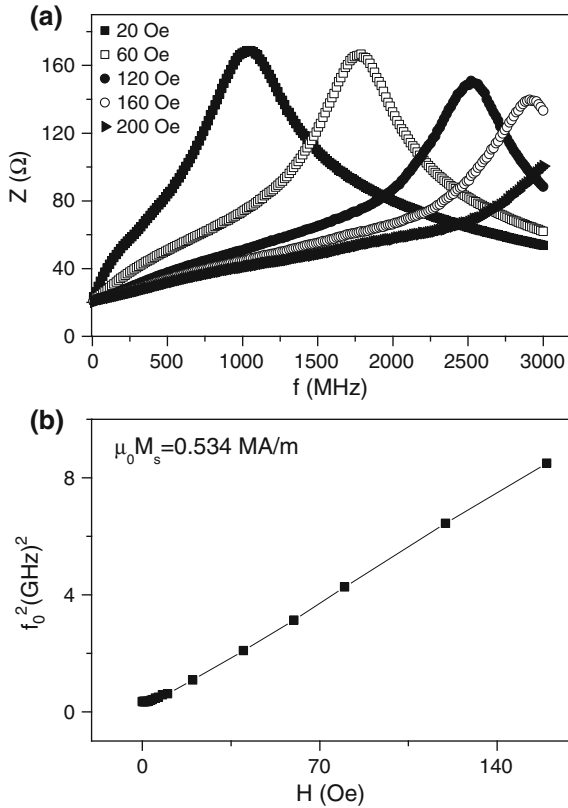


Fig. 9 Frequency dependence of GMI effect (a) and $f_0^2(H)$ dependence (b) measured for $\text{Co}_{67.05}\text{Fe}_{3.85}\text{Ni}_{1.4}\text{B}_{11.33}\text{Si}_{14.47}\text{Mo}_{1.69}$ microwires with $d \approx 21.4 \mu\text{m}$, $\rho \approx 0.816$. Reprinted with permission from Ref. [21] DOI 10.1007/s10948-012-1962-x, Copyright (2013) with permission from Springer (Fig. 4c, d)

4 Effect of Partial Crystallization and Nanocrystallization on Magnetic Properties and GMI

Although the crystallization of amorphous materials usually results in a degradation of their magnetic softness, in some cases the crystallization can improve its magnetically soft behaviour. This is the case of so-called “nanocrystalline” alloys obtained by suitable annealing of amorphous metals. These materials have been introduced in 1988 by Yoshizawa et al. [30], and later they have been intensively studied by a number of research groups [31–34]. As was mentioned in the introduction, the nanocrystalline structure of a partially crystalline amorphous precursor is observed particularly in Fe-Si-B alloys with small additions of Cu and Nb. Small additions of Cu and Nb allow inhibiting of the grains nucleation and decreasing of the grain growth rate [30–33]. The main interest in such nanocrystalline alloys is

related to extremely soft magnetic properties combined with a high saturation magnetization. Such soft magnetic character is thought to be originated because the magnetocrystalline anisotropy vanishes and the very small magnetostriction achieved value when the grain size approaches 10 nm [30–33].

Previously, a considerable magnetic softening and enhancement of GMI effect has been reported for Finemet-type ribbons, conventional wires [52] and glass-coated Finemet-type microwires [53–57]. But the most considerable improvement of GMI effect in the case of glass-coated microwires is reported quite recently [34–37].

As-prepared Finemet-type $\text{Fe}_{73.4}\text{Cu}_1\text{Nb}_{3.1}\text{Si}_x\text{B}_{22.5-x}$ ($x = 11.5, 13.5$ and 16.5) and $\text{Fe}_{73.4-x}\text{Cu}_1\text{Nb}_{3.1}\text{Si}_{13.4+x}\text{B}_{9.1}$ ($0 \leq x \leq 1.1$) microwires present rectangular bistable hysteresis loops similarly to other Fe-rich amorphous microwires [34–37]. For illustration in Fig. 10a we provide hysteresis loops of $\text{Fe}_{70.8}\text{Cu}_1\text{Nb}_{3.1}\text{Si}_{14.5}\text{B}_{10.6}$ microwires with different ρ -ratios ($\rho = 0.67$ and $\rho = 0.38$).

The coercivity, H_c , of as-prepared Finemet-type microwires depends on the ratio $\rho = d/D$ (Fig. 10b).

Fig. 10 Hysteresis loops (a) and $H_c(\rho)$ dependence (b) of $\text{Fe}_{70.8}\text{Cu}_1\text{Nb}_{3.1}\text{Si}_{14.5}\text{B}_{10.6}$ as-prepared microwires. Reprinted with permission from [57] Copyright © 2014, with permission from Springer DOI: [10.1007/s11664-014-3370-4](https://doi.org/10.1007/s11664-014-3370-4) (Fig. 5)

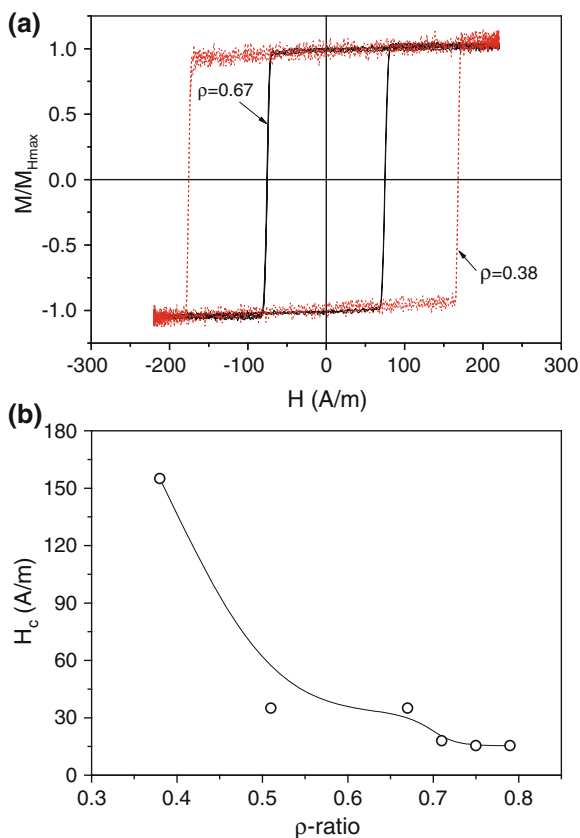


Figure 11a–c present XRD spectra of some selected as-prepared $\text{Fe}_{70.8}\text{Cu}_1\text{Nb}_{3.1}\text{Si}_{16}\text{B}_{9.1}$, $\text{Fe}_{70.8}\text{Cu}_1\text{Nb}_{3.1}\text{Si}_{14.5}\text{B}_{10.6}$ and $\text{Fe}_{73.8}\text{Cu}_1\text{Nb}_{3.1}\text{Si}_{13}\text{B}_{9.1}$ microwires.

The first two peaks of the XRD spectra between 10° and 30° correspond to the glass layer and the other peaks at above 40° are related to the metallic nucleus. All $\text{Fe}_{70.8}\text{Cu}_1\text{Nb}_{3.1}\text{Si}_{16}\text{B}_{9.1}$ and $\text{Fe}_{70.8}\text{Cu}_1\text{Nb}_{3.1}\text{Si}_{14.5}\text{B}_{10.6}$ samples present a completely amorphous structure (Fig. 11a, b).

But some of $\text{Fe}_{73.8}\text{Cu}_1\text{Nb}_{3.1}\text{Si}_{13}\text{B}_{9.1}$ microwires (see Fig. 11c) present a partially crystalline structure already in the as-prepared state.

Usually, the basic method to obtain a nanocrystalline structure from the amorphous state is achieving the crystallization of amorphous matrix by an appropriate heat treatment.

As-prepared samples have been annealed at different annealing temperatures, T_{ann} , at a fixed annealing time. Annealing results show considerable changes of the structure and magnetic properties.

Starting from T_{ann} ranging from 550 to 650 °C a main crystalline peak is appearing in the range between 42° and 45° which correspond to the existence of α -Fe (Si) BCC crystal structure [30–33], as well as another two weak peaks appearing in the range between 65° and 85° (Fig. 12a). However, in the case of the $\text{Fe}_{73.8}\text{Cu}_1\text{Nb}_{3.1}\text{Si}_{13}\text{B}_{9.1}$ microwire such crystalline peak has been observed in the as-prepared state (Fig. 11c) and, consequently after annealing (Fig. 12b). Increasing the annealing temperature, T_{ann} , this peak becomes higher and narrower which indicates an increase in both the bcc-Fe phase volume fraction and grain size growth, respectively.

The shape of the crystalline peak, particularly its width, contains useful information on the average grain size of the corresponding crystalline phase. Considering the main crystalline peak, by estimating the width of the peak, ϵ , as well as the crystallization angle, 2θ , then by substituting these parameters on the Debye-Scherrer equation (Eq. 12), one can obtain the value of the grain size (D).

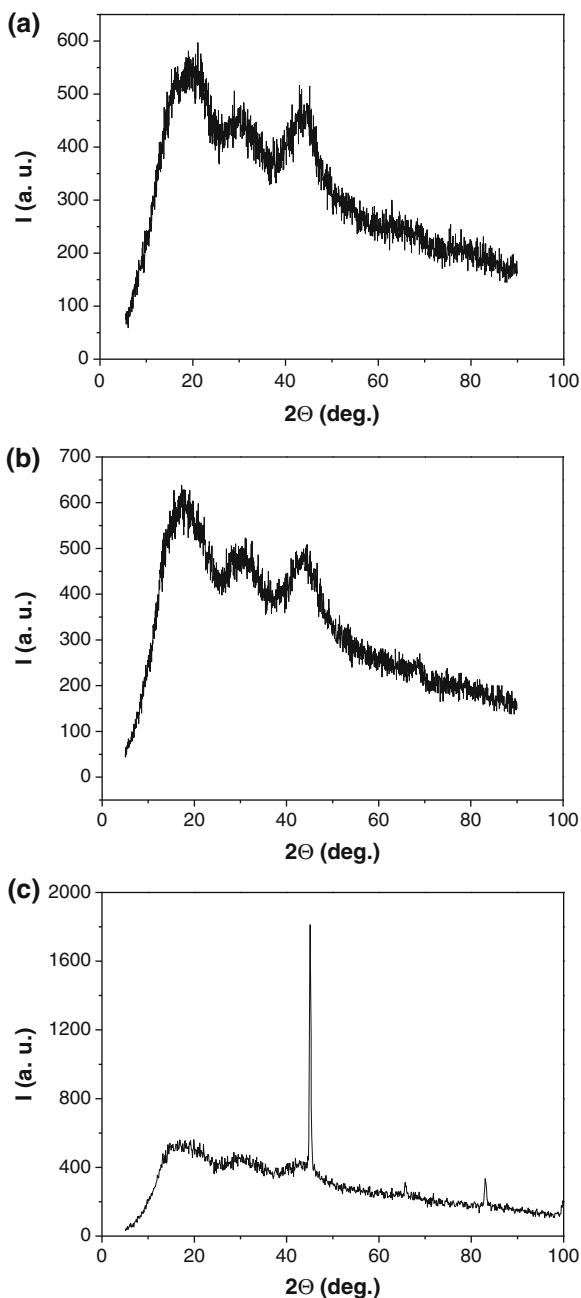
$$D = k\lambda / \epsilon \cos 2\theta \quad (12)$$

where, ϵ is the half height width of the crystalline peak and 2θ is the angular position of the maximum crystalline peak. We found that the average grain size in the range of 550 °C $\leq T_{\text{ann}} \leq 600$ °C is between 12 and 17 nm. By increasing at $T_{\text{ann}} \geq 650$ °C, D rapidly increases achieving values above 30 nm (see Fig. 13).

It is worth mentioning that not only the average grain size, but also the volume fraction of precipitating nanocrystalline phase affects the physical properties of devitrified materials [31, 32].

A strong dependence of magnetic properties on the sample's geometry in the as-prepared state has been observed for all compositions. Hysteresis loops (plotted as the normalized magnetization M/M_{Hmax} versus applied magnetic field H) of as-prepared microwires present rectangular shape typical for amorphous Fe-rich microwires (Figs. 10a and 14). As can be appreciated from Fig. 10b the coercivity,

Fig. 11 XRD patterns of as-prepared microwires: $\text{Fe}_{70.8}\text{Cu}_1\text{Nb}_{3.1}\text{Si}_{16}\text{B}_{9.1}$ with $\rho = 0.75$ (a), $\text{Fe}_{70.8}\text{Cu}_1\text{Nb}_{3.1}\text{Si}_{14.5}\text{B}_{10.6}$ with $\rho = 0.81$ (b) and $\text{Fe}_{73.8}\text{Cu}_1\text{Nb}_{3.1}\text{Si}_{13}\text{B}_{9.1}$ with $\rho = 0.6$ (c). Reprinted with permission from [57] Copyright © 2014, with permission from Springer DOI: [10.1007/s11664-014-3370-4](https://doi.org/10.1007/s11664-014-3370-4) (Fig. 1)



H_c is drastically affected by the ρ -ratio. Strong $H_c(\rho)$ dependence can be explained taking into account the influence of the internal stresses on the coercivity. As was mentioned above the strength of internal stresses is a function of ρ -ratio.

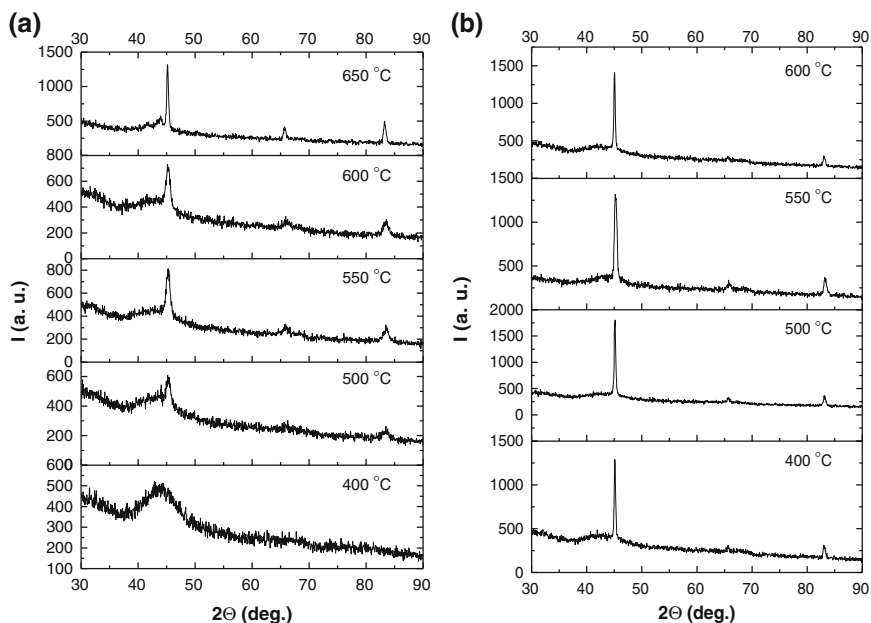


Fig. 12 XRD patterns of annealed microwires $\text{Fe}_{70.8}\text{Cu}_1\text{Nb}_{3.1}\text{Si}_{14.5}\text{B}_{10.6}$ with $\rho = 0.81$ (a) and $\text{Fe}_{73.8}\text{Cu}_1\text{Nb}_{3.1}\text{Si}_{13}\text{B}_{9.1}$ with $\rho = 0.6$ (b). Annealing temperatures are indicated within each pattern. (a) Reprinted with permission from [57] Copyright © 2014, with permission from Springer DOI: [10.1007/s11664-014-3370-4](https://doi.org/10.1007/s11664-014-3370-4) (Fig. 2)

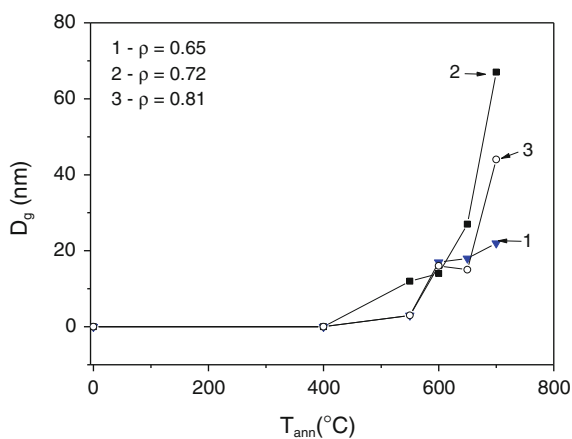
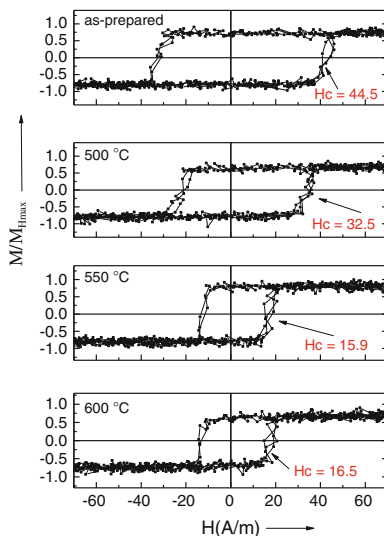


Fig. 13 Dependence of average grain size on annealing temperature for $\text{Fe}_{70.8}\text{Cu}_1\text{Nb}_{3.1}\text{Si}_{14.5}\text{B}_{10.6}$ microwires with various ρ -ratios. Reprinted with permission from [57] Copyright © 2014, with permission from Springer DOI: [10.1007/s11664-014-3370-4](https://doi.org/10.1007/s11664-014-3370-4) (Fig. 3)

Fig. 14 Hysteresis loops of as-prepared and annealed $\text{Fe}_{70.8}\text{Cu}_1\text{Nb}_{3.1}\text{Si}_{14.5}\text{B}_{10.6}$ microwires, with $\rho = 0.81$, at different temperatures measured at fixed magnetic field amplitude of 225 A/m. Reprinted with permission from [57] Copyright © 2014, with permission from Springer DOI: 10.1007/s11664-014-3370-4 (Fig. 6)



Hysteresis loops of as-prepared and annealed $\text{Fe}_{70.8}\text{Cu}_1\text{Nb}_{3.1}\text{Si}_{14.5}\text{B}_{10.6}$ microwires ($\rho = 0.81$) at different temperatures are presented in Fig. 14. It is worth mentioning, that the coercivity decreases upon increasing the annealing temperature, while the rectangular character of hysteresis loops is observed for all samples even annealed at below certain temperature.

In Fig. 15 we plotted the coercivity dependence on the annealing temperature for $\text{Fe}_{70.8}\text{Cu}_1\text{Nb}_{3.1}\text{Si}_{14.5}\text{B}_{10.6}$ glass-coated microwire with different ρ -ratio.

According to these data, a tendency towards decreasing H_c values is observed at the range of 500–550 °C. Above $T_{\text{ann}} \approx 600$ °C the magnetic bistability disappears (hysteresis loops cannot be considered perfectly rectangular). A similar behavior associated with the devitrification and magnetic softening has been previously reported in other Finemet-type microwires [53].

The dependence of the coercivity H_c on the metallic nucleus diameter (d), is in agreement with the previously reported dependence for Fe-Si-B-C amorphous microwires [26]. Hence, the coercivity increasing with the decreasing of the metallic nucleus diameter is interpreted as the interplay of internal stresses and demagnetizing factor.

It is worth mentioning that internal stresses induced by the glass coating affect not only magnetic properties of as-prepared microwires but also the nanocrystallization process. Thus, previously we have studied $H_c(T_{\text{ann}})$ dependences in microwires with rather different ρ -ratios and reported that the internal stresses induced by the glass coating affect the dependence of coercivity on the annealing temperature [56]. We have explained the considerable observed differences in $H_c(T_{\text{ann}})$ considering that internal stresses hinder the segregation of FeB phases responsible of the magnetic hardening.

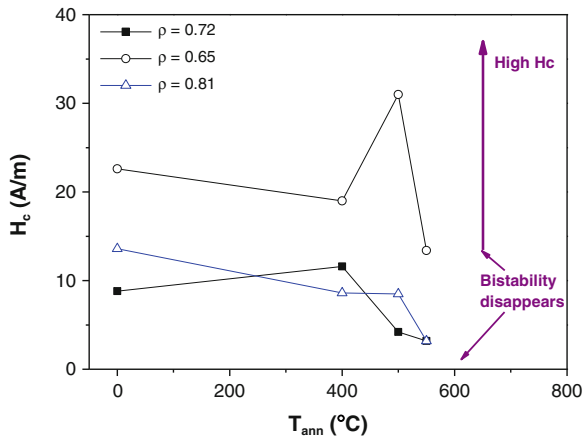


Fig. 15 Dependence of the coercivity, H_c , for the $\text{Fe}_{70.8}\text{Cu}_1\text{Nb}_{3.1}\text{Si}_{14.5}\text{B}_{10.6}$ glass-coated microwire with selected ρ -ratio on annealing temperature. Reprinted with permission from [57] Copyright © 2014, with permission from Springer DOI: [10.1007/s11664-014-3370-4](https://doi.org/10.1007/s11664-014-3370-4) (Fig. 7)

Consequently, a magnetic softening with the lowest value of coercivity and switching field is obtained in the samples treated at 500–600 °C, which could be ascribed to the fact that the first crystallization process has been developed leading to fine α -Fe (Si) nanocrystals with grain size around 10–20 nm (compare Figs. 12, 14 and 15). This behavior is similar to that one widely reported for FINEMET ribbons [30–33].

GMI ration has been measured in as-prepared and annealed samples. As it was expected, samples with amorphous structure in the as-prepared state exhibit a rather small GMI effect (below 5 % see Fig. 16) similar to other Fe-based glass-coated microwires with positive magnetostriction. In contrast, nanocrystalline $\text{Fe}_{70.8}\text{Cu}_1\text{Nb}_{3.1}\text{Si}_{16}\text{B}_{9.1}$ microwires annealed at 550 °C exhibit higher GMI effect ($\Delta Z/Z \approx 90$ %, see Fig. 16).

Indeed, like all Fe-based microwires, studied Fe-Cu-Nb-Si-B microwires exhibit a high positive magnetostriction. Consequently, the stress distribution arising from simultaneous rapid quenching of metallic nucleus inside the glass coating must result in a longitudinal magnetization easy axis [26]. The resulting domain structure (with a low circular magnetic permeability typical for magnetically bistable samples) usually exhibits a small GMI effect. Therefore, the GMI effect in the as-prepared FINEMET microwires with positive magnetostriction is low.

A noticeable change in the GMI has been observed after the appearance of nanocrystallites (Fig. 16). As discussed elsewhere, after the nanocrystallization the average magnetostriction constant takes nearly- zero values [31, 32] thanks to the control of the crystalline volume fraction:

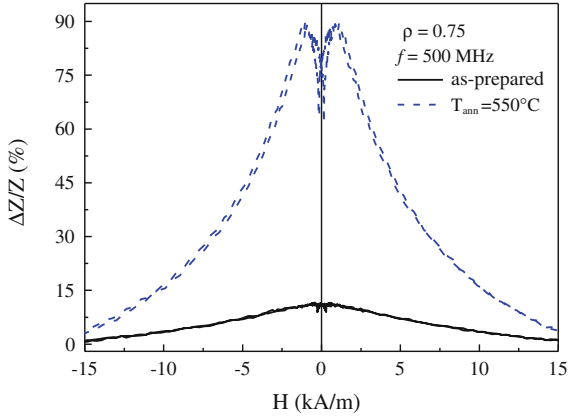


Fig. 16 Effect of annealing at 550 °C for 1 h on $\Delta Z/Z(H)$ dependence of $\text{Fe}_{70.8}\text{Cu}_1\text{Nb}_{3.1}\text{Si}_{16}\text{B}_{9.1}$ microwire with $\rho = 0.75$ measured at 500 MHz in comparison with the GMI response of the as-prepared sample. Reprinted with permission from [57] Copyright © 2014, with permission from Springer DOI: [10.1007/s11664-014-3370-4](https://doi.org/10.1007/s11664-014-3370-4) (Fig. 8)

$$\lambda_{s,\text{eff}} = V_{\text{cr}}\lambda_{s,\text{cr}} + (1 - V_{\text{cr}})\lambda_{s,\text{am}} \quad (13)$$

being $\lambda_{s,\text{eff}}$ the saturation magnetostriction coefficient and V_{cr} the crystalline volume fraction.

As discussed elsewhere, the GMI effect is affected by the magnetic anisotropy [5, 17]. Consequently, the shape of $\Delta Z/Z(H)$ dependence and maximum GMI ratio $\Delta Z/Z_{\text{max}}$ are considerably affected by annealing [17].

It should be noted that the GMI response is affected by the frequency and can be optimized choosing the appropriate driving frequency [26]. As was mentioned above, the variation of the skin effect of a magnetic conductor under an applied magnetic field is the main origin of the GMI effect [1, 2]. The skin depth, δ , of magnetic conductor is given by Eq. (4) being f the frequency of the current, σ the electrical conductivity of the material, and $\mu\phi$ the circular magnetic permeability as a parameters.

One of the conditions for the observation of the GMI effect is that the skin depth must be reduced below the wire radius. Despite this, the frequency at which the maximum GMI value is obtained depends strongly on the sample geometry, i.e., on the ρ -ratio [26].

Frequency dependences of $\Delta Z/Z_{\text{max}}$ obtained in $\text{Fe}_{70.8}\text{Cu}_1\text{Nb}_{3.1}\text{Si}_{16}\text{B}_{9.1}$ microwires with different ρ -ratios are displayed in Fig. 17. Similarly to amorphous Co-rich microwires one can conclude that $\Delta Z/Z$ and its frequency dependence are strongly affected by the magnetoelastic anisotropy determined by the ρ -ratio.

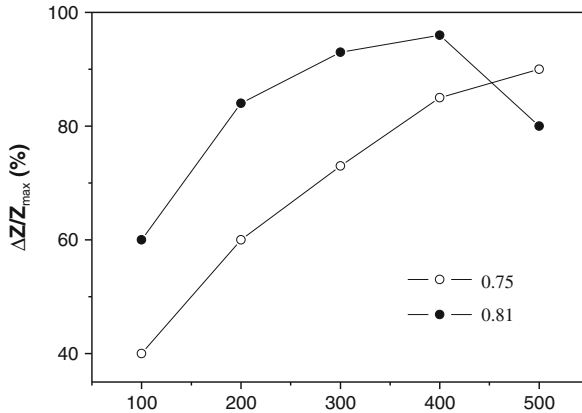


Fig. 17 Frequency dependence of $\text{Fe}_{70.8}\text{Cu}_1\text{Nb}_{3.1}\text{Si}_{16}\text{B}_{9.1}$ microwires annealed at $550\text{ }^\circ\text{C}$ with different geometric ratios ρ . Reprinted with permission from [57] Copyright © 2014, with permission from Springer DOI: [10.1007/s11664-014-3370-4](https://doi.org/10.1007/s11664-014-3370-4) (Fig. 9)

5 Conclusion

Studies of magnetic properties and GMI effect of amorphous Co-Fe rich microwires reveal that selecting its appropriate chemical composition and geometry they present GMI effect at GHz frequencies. Hysteresis loops and magnetic field dependences of GMI effect are affected by the magnetoelastic anisotropy. Features of high frequency GMI effect can be described using a FMR-like approximation.

Investigations of magnetic properties of Finemet-type Fe-Cu-Nb-Si-B microwires reveal that annealing considerably affects the hysteresis loops and GMI effect of this family of microwires. In as-prepared microwires, the reduction of the ρ -ratio results in the rise of coercivity. Magnetoelastic anisotropy affects soft magnetic properties of as-prepared FeCuNbSiB microwires. We observed magnetic softening and a considerable increasing of the GMI effect in Finemet-type FeCuNbSiB with nanocrystalline structure even in as-prepared microwires. After an adequate annealing of Finemet-type microwires we observed a GMI ratio of about 100 %. The nanocrystallization of FeCuNbSiB microwires is a key factor for the optimization of the GMI effect.

References

1. L.V. Panina, K. Mohri, Magneto-impedance effect in amorphous wires. *Appl. Phys. Lett.* **65**, 1189–1191 (1994)
2. R.S. Beach, A.E. Berkowitz, Giant magnetic-field dependent impedance of amorphous FeCoSiB wire. *Appl. Phys. Lett.* **64**(26), 3652 (1994)

3. E.P. Harrison, G.L. Turney, H. Rowe, H. Gollop, The electrical properties of high permeability wires carrying alternating current. *Proc. R. Soc. Lond. A* **157**, 451–479 (1936)
4. A. Zhukov, V. Zhukova, *Magnetic Sensors Based on Thin Magnetically Soft Wires with Tuneable Magnetic Properties and Its Applications*. International Frequency Sensor Association (IFSA) Publishing, Ronda de Ramon Otero Pedrayo, 42C, 1-5, 08860, Castelldefels (Barcelona), Spain (2014). ISBN-10: 84-617-1866-6
5. N.A. Usov, A.S. Antonov, A.N. Lagar'kov, Theory of giant magneto-impedance effect in amorphous wires with different types of magnetic anisotropy. *J. Magn. Magn. Mater.* **8**, 159, 185 (1998)
6. P. Ciureanu, G. Rudkowska, L. Clime, A. Sklyuyev, A. Yelon, Anisotropy optimization of giant magnetoimpedance sensors. *J. Optoelectron. Adv. Mater.* **6**, 905–910 (2004)
7. A. Zhukov, M. Ipatov, M. Churyukanova, S. Kaloshkin, V. Zhukova, Giant magnetoimpedance in thin amorphous wires: from manipulation of magnetic field dependence to industrial applications. *J. Alloys Comp.* **586**(Suppl. 1), S279–S286 (2014). doi:[10.1016/j.jallcom.2012.10.082](https://doi.org/10.1016/j.jallcom.2012.10.082)
8. M.E. McHenry, M.A. Willard, D.E. Laughlin, Amorphous and nanocrystalline materials for applications as soft magnets. *Prog. Mater. Sci.* **44**, 291 (1999)
9. Y. Honkura, Development of amorphous wire type MI sensors for automobile use. *J. Magn. Magn. Mater.* **249**, 375–381 (2002)
10. K. Mohri, T. Uchiyama, L.P. Shen, C.M. Cai, L.V. Panina, Amorphous wire and CMOS IC-based sensitive micro-magnetic sensors (MI sensor and SI sensor) for intelligent measurements and controls. *J. Magn. Magn. Mater.* **249**, 351–356 (2002)
11. D.P. Makhnovskiy, L.V. Panina, D.J. Mapps, Field-dependent surface impedance tensor in amorphous wires with two types of magnetic anisotropy: helical and circumferential. *Phys. Rev. B* **63**, 1444241 (2001)
12. S.I. Sandacci, D.P. Makhnovskiy, L.V. Panina, K. Mohri, Y. Honkura, Off-diagonal impedance in amorphous wires and its application to linear magnetic sensors. *IEEE Trans. Magn.* **35**, 3505–3510 (2004)
13. P. Aragonese, A. Zhukov, J. Gonzalez, J.M. Blanco, L. Dominguez, Effect of AC driving current on magneto-impedance effect. *Sensors Actuators A* **81**(1–3), 86–90 (2000)
14. A. Zhukov, M. Ipatov, V. Zhukova, C. Garcia, J. Gonzalez, J.M. Blanco, Development of ultra-thin glass-coated amorphous microwires for HF magnetic sensor applications. *Phys. Stat. Sol. (A)* **205**(6), 1367–1372 (2008). doi:[10.1002/pssa.200778133](https://doi.org/10.1002/pssa.200778133)
15. K.R. Pirota, L. Kraus, H. Chiriac, M. Knobel, Magnetic properties and GMI in a CoFeSiB glass-covered microwire. *J. Magn. Magn. Mater.* **21**, L243–L247 (2000)
16. V. Zhukova, A. Chizhik, A. Zhukov, A. Torcunov, V. Larin, J. Gonzalez, Optimization of giant magneto-impedance in Co-rich amorphous microwires. *IEEE Trans. Magn.* **38**(5, Part I), 3090–3092 (2002)
17. J.M. Blanco, A. Zhukov, J. Gonzalez, Effect of tensile and torsion on GMI effect in amorphous wire. *J. Magn. Magn. Mater.* **196–197**, 377–379 (1999)
18. V. Zhukova, M. Ipatov, J. González, J.M. Blanco, A.P. Zhukov, Development of thin microwires with enhanced magnetic softness and GMI. *IEEE Trans. Magn.* **44**(Part 2), 3958–3961 (2008)
19. M.-H. Phan, H.-X. Peng, Giant magnetoimpedance materials: fundamentals and applications. *Prog. Mater. Sci.* **53**, 323–420 (2008)
20. D. Ménard, M. Britel, P. Ciureanu, A. Yelon, Giant magnetoimpedance in a cylindrical conductor. *J. Appl. Phys.* **84**, 2805–2814 (1998)
21. A. Zhukov, M. Ipatov, C. Garcia, M. Churyukanova, S. Kaloshkin, V. Zhukova, From manipulation of giant magnetoimpedance in thin wires to industrial applications. *J. Supercond. Nov. Magn.* **26**, 1045–1054 (2013)
22. T. Uchiyama, K. Mohri, Sh Nakayama, Measurement of spontaneous oscillatory magnetic field of Guinea-Pig smooth muscle preparation using pico-tesla resolution amorphous wire magneto-impedance sensor. *IEEE Trans. Magn.* **47**(10), 3070–3073 (2011)

23. V.S. Larin, A.V. Torcunov, A. Zhukov, J. González, M. Vazquez, L. Panina, Preparation and properties of glass-coated microwires. *J. Magn. Magn. Mater.* **249**(1-2), 39–45 (2002)
24. Y. Konno, K. Mohri, Magnetostriction measurements for amorphous wires. *IEEE Trans. Magn.* **25**, 3623–3625 (1989)
25. A. Zhukov, V. Zhukova, J.M. Blanco, A.F. Cobeño, M. Vazquez, J. Gonzalez, Magnetostriction in glass-coated magnetic microwires. *J. Magn. Magn. Mater.* **258–259**, 151–157 (2003)
26. V. Zhukova, M. Ipatov, A. Zhukov, Thin magnetically soft wires for magnetic microsensors. *Sensors* **9**, 9216–9240 (2009). doi:[10.3390/s91109216](https://doi.org/10.3390/s91109216)
27. J. Velázquez, M. Vazquez, A. Zhukov, Magnetoelastic anisotropy distribution in glass-coated microwires. *J. Mater. Res.* **11**, 2499–2505 (1996)
28. A.S. Antonov, V.T. Borisov, O.V. Borisov, A.F. Prokoshin, N.A. Usov, Residual quenching stresses in glass-coated amorphous ferromagnetic microwires. *J. Phys. D Appl. Phys.* **33**, 1161–1168 (2000)
29. H. Chiriac, T.-A. Ovari, A. Zhukov, Magnetoelastic anisotropy of amorphous microwires. *J. Magn. Magn. Mater.* **254–255**, 469–471 (2003)
30. Y. Yoshizawa, S. Oguma, K. Yamauchi, New Fe-based soft magnetic alloys composed of ultrafine grain structure. *J. Appl. Phys.* **64**, 6044 (1988)
31. Y. Yoshizawa, K. Yamauchi, Fe-based soft magnetic alloy composed of ultrafinegrain structure. *Mater. Trans. JIM* **31**, 307–314 (1990)
32. G. Herzer, Grain size dependence of coercivity and permeability in nanocrystalline ferromagnets. *IEEE Trans. Magn.* **26**, 1397–1402 (1990)
33. G. Herzer, Anisotropies in soft magnetic nanocrystalline alloys. *J. Magn. Magn. Mater.* **294**, 99–106 (2005)
34. A. Talaat, M. Ipatov, V. Zhukova, J.M. Blanco, M. Churyukanova, S. Kaloshkin, A. Zhukov, Giant magneto-impedance effect in thin Finemet nanocrystalline microwires. *Phys. Status Solidi C* **11**(5–6), 1120–1124 (2014)
35. A.P. Zhukov, A. Talaat, M. Ipatov, J.M. Blanco, L. Gonzalez-Legarreta, B. Hernando, V. Zhukova, Effect of nanocrystallization on magnetic properties and GMI effect of microwires. *IEEE Trans. Magn.* **50**(6), 2501905 (2014)
36. A. Zhukov, M. Ipatov, A. Talaat, M. Churyukanova, S. Kaloshkin, V. Zhukova, Giant magnetoimpedance in thin amorphous and nanocrystalline microwires. *Appl. Phys. A Mater. Sci. Process.* **115**, 547–553 (2014)
37. A. Talaat, V. Zhukova, M. Ipatov, J.J. del Val, L. Gonzalez-Legarreta, B. Hernando, J.M. Blanco, A. Zhukov, Effect of nanocrystallization on giant magnetoimpedance effect of Fe based microwires. *Intermetallics* **51**, 59–63 (2014)
38. A. Talaat, V. Zhukova, M. Ipatov, J.M. Blanco, L. Gonzalez-Legarreta, B. Hernando, J.J. del Val, J. Gonzalez, A. Zhukov, Optimization of the giant magnetoimpedance effect of Finemet-type microwires through the nanocrystallization. *J. Appl. Phys.* **115**, 17A313 (2014)
39. A.V. Ulitovski, N.M. Avernin, Method of fabrication of metallic microwire. Patent No 161325 (USSR), 19.03.64. Bulletin, No 7, p. 14
40. A.V. Ulitovsky, I.M. Maianski, A.I. Avramenco, Method of continuous casting of glass coated microwire. Patent No 128427 (USSR), 15.05.60. Bulletin, No 10, p. 14
41. E.Ya. Badinter, N.R. Berman, I.F. Drabenko, V.I. Zaborovsky, Z.I. Zelikovsky, V.G. Cheban, Cat microwires and its properties. Shtinica, Kishinev (1973)
42. L. Kraus, J. Schneider, H. Wiesner, Ferromagnetic resonance in amorphous alloys prepared by rapid quenching from the melt. *Czech J. Phys.* **26**(5), 601–602 (1976)
43. A. Zhukov, V. Zhukova, Magnetic properties and applications of ferromagnetic microwires with amorphous and nanocrystalline structure. Nova Science Publishers, New York (2009). ISBN:978-1-60741-770-5
44. A. Zhukov, E. Kostitsyna, E. Shuvaeva, S. Kaloshkin, M. Churyukanova, V. Sudarchikova, A. Talaat, V. Zhukova, Effect of composite origin on magnetic properties of glass-coated microwires. *Intermetallics* **44**, 88–93 (2014). doi:[10.1016/j.intermet.2013.08.014](https://doi.org/10.1016/j.intermet.2013.08.014)

45. A. Zhukov, A. Talaat, M. Ipatov, J.J. del Val, L. Gonzalez-Legarreta, B. Hernando, A. Chizhik, J.M. Blanco, V. Zhukova, Optimization of magnetic properties and giant magnetoimpedance effect in nanocrystalline microwires. *J. Supercond. Nov. Magn.* **28**, 813–822 (2015). doi:[10.1007/s10948-014-2654-5](https://doi.org/10.1007/s10948-014-2654-5)
46. A. Zhukov, A. Talaat, M. Ipatov, V. Zhukova, High frequency giant magnetoimpedance effect of amorphous microwires for magnetic sensors applications. *Int. J. Smart Sens. Intell. Syst.* (2014). In: Proceedings of the 8th international conference on sensing technology, 2–4 Sep 2014, Liverpool, UK, pp 624-629. <http://www.s2is.org>
47. M. Ipatov, V. Zhukova, A. Zhukov, J. Gonzalez, A. Zvezdin, Low-field hysteresis in the magnetoimpedance of amorphous microwires. *Phys. Rev. B* **81**, 134421 (2010)
48. A. Zhukov, M. Ipatov, V. Zhukova, Amorphous microwires with enhanced magnetic softness and GMI characteristics. *EPJ Web Conf.* **29**, 00052 (2012)
49. A.F. Cobeño, A. Zhukov, J.M. Blanco, J. Gonzalez, Giant magneto-impedance effect in CoMnSiB amorphous microwires. *J. Magn. Magn. Mater.* **234**, L359–L365 (2001)
50. C. García, A. Zhukov, V. Zhukova, M. Ipatov, J.M. Blanco, J. Gonzalez, Effect of tensile stresses on GMI of Co-rich amorphous microwires. *IEEE Trans. Magn.* **41**, 3688–3690 (2005)
51. A. Zhukov, A. Talaat, M. Ipatov, V. Zhukova, Tailoring of high frequency giant magnetoimpedance effect of amorphous Co-rich microwires. *IEEE Magn. Lett.* (2015) (accepted). doi:[10.1109/LMAG.2015.2397877](https://doi.org/10.1109/LMAG.2015.2397877)
52. H.Q. Guo, H. Kronmüller, T. Dragon, Z.H. Cheng, B.G. Shen, Influence of nanocrystallization on the evolution of domain patterns and the magnetoimpedance effect in amorphous $\text{Fe}_{73.5}\text{Cu}_1\text{Nb}_3\text{Si}_{13.5}\text{B}_9$ ribbons. *J. Appl. Phys.* **89**, 514 (2001)
53. J. Arcas, C. Gómez-Polo, A. Zhukov, M. Vázquez, V. Larin, A. Hernando, Magnetic properties of amorphous and devitrified FeSiBCuNb glass-coated microwires. *Nanostruct. Mater.* **7**(8), 823 (1996)
54. C. Dudek, A.L. Adenot-Engelvin, F. Bertin, O. Acher, J. Non-Cryst. Solids **353**, 925 (2007)
55. H. Chiriac, T.A. Ovari, C.S. Marinescu, Giant magneto-impedance effect in nanocrystalline glass-covered wires. *J. Appl. Phys.* **83**, 6584 (1998)
56. V. Zhukova, A.F. Cobeño, A. Zhukov, J.M. Blanco, V. Larin, J. Gonzalez, Coercivity of glass-coated $\text{Fe}_{73.4-x}\text{Cu}_1\text{Nb}_{3.1}\text{Si}_{13.4+x}\text{B}_{9.1}$ ($0 \leq x \leq 1.6$) microwires. *Nanostruct. Mater.* **11**(8), 1319–1327 (1999)
57. V. Zhukova, A. Talaat, M. Ipatov, J.J. del Val, L. Gonzalez-Legarreta, B. Hernando, A. Zhukov, Effect of nanocrystallization on magnetic properties and GMI effect of Fe-rich microwires. *J. Electron. Mater.* **43**(12) (2014). doi:[10.1007/s11664-014-3370-4](https://doi.org/10.1007/s11664-014-3370-4)